Journal of Loss Prevention in the Process Industries 92 (2024) 105479

Contents lists available at ScienceDirect

Journal of Loss Prevention in the Process Industries

journal homepage: www.elsevier.com/locate/jlp

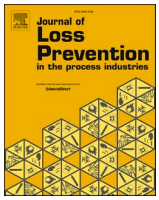

Laminar burning velocity of ethanol-ethyl acetate mixtures in air

Ernesto Salzano [a,b], Benedetta Anna De Liso [a], Francesco Cammarota [b], Valeria Di Sarli [b,*]

[a] Dipartimento di Ingegneria Civile, Chimica, Ambientale e dei Materiali, Alma Mater Studiorum - Università di Bologna, Via Umberto Terracini 28, 40131, Bologna, Italy
[b] Istituto di Scienze e Tecnologie per l'Energia e la Mobilità Sostenibili (STEMS), Consiglio Nazionale delle Ricerche (CNR), Via Guglielmo Marconi 4, 80125, Napoli, Italy

ARTICLE INFO

Keywords:
Ethanol-ethyl acetate mixtures
Laminar burning velocity
Detailed chemical kinetic calculations
Closed vessel explosion experiments
Le Chatelier's mixing rule

ABSTRACT

Alcohols, esters, and their mixtures are ubiquitous in the process industry. However, safety data remain limited, especially for mixtures. In this work, the laminar burning velocity, S_l, of ethanol-ethyl acetate mixtures in air was investigated (at 90 °C and atmospheric pressure) through computations performed using three different detailed chemical kinetic mechanisms, and measurements obtained from pressure time histories recorded during closed vessel explosion experiments. Computations were run varying the equivalence ratio, φ, from 0.6 to 1.7, and the mole fraction of ethanol in the fuel mixture from 0 (only ethyl acetate) to 1 (only ethanol). For all systems, explosion experiments were carried out at $\varphi = 1.1$, i.e., the composition at which, according to calculations, S_l achieves its maximum value. Regardless of the kinetic mechanism, reasonable agreement is found between computed and experimental data, including experimental data retrieved from the literature for ethanol and ethyl acetate. Results show that the behavior of ethanol-ethyl acetate is bounded between the behaviors of ethanol and ethyl acetate, approaching the former/latter as the mixture is enriched in ethanol/ethyl acetate. Over the whole range of equivalence ratios explored, the values of S_l for ethanol-ethyl acetate are smaller than those obtained by averaging the corresponding values of ethanol and ethyl acetate according to their mole proportions in the fuel mixture. This is also confirmed experimentally. A simple Le Chatelier's mixing rule-like formula is proved to predict values of S_l that closely match both computed and experimental data, suggesting that the nature of the interaction between ethanol and ethyl acetate is predominantly thermal rather than chemical.

1. Introduction

The broad spectrum of applications of ethanol, ethyl acetate, and ethanol-ethyl acetate mixtures includes their use as fuels or fuel additives, and as crucial solvents in pharmaceuticals as well as in paints, inks, coatings, and adhesives. In addition, ethanol-ethyl acetate mixtures are a valid alternative to Folch reagent for extracting animal lipids (thus avoiding the use of chloroform) (Lin et al., 2004). Despite their multifaceted utility, the intrinsic flammability of these systems necessitates meticulous safety considerations throughout their lifecycle, from production to storage and utilization. Indeed, the relatively low flash point of ethanol and ethyl acetate — 12.8 °C and −4.4 °C, respectively (Crowl, 2003) — makes them highly prone to generating explosive conditions.

Research endeavors have aimed to predict the flash point of multicomponent flammable mixtures, emphasizing the criticality of comprehensive safety assessments across industrial domains. Notably, investigations into ethanol-ethyl acetate mixtures have revealed intriguing synergistic effects across different compositions leading to the so called "minimum flash point behavior". When this behavior occurs, the flash point of the mixtures decreases below that of their constituents (Di Benedetto et al., 2018a, 2018b). This behavior intensifies the explosion hazard associated with ethanol-ethyl acetate mixtures compared to the individual components. Hence, dedicated investigations on the combustion/explosion behavior of such mixtures are imperative to elucidate their safety implications. For ethanol and, mostly, ethyl acetate, the lack of data mainly concerns explosion characteristics other than laminar burning velocity (Cammarota et al., 2012; Li et al., 2015; Mitu and Brandes, 2017; Xu et al., 2020a; Oppong et al., 2021a; Ning et al., 2023). Conversely, for ethanol-ethyl acetate mixtures, there also exists a substantial absence of information concerning this parameter (Cammarota et al., 2022; Liu et al., 2022).

The laminar burning velocity, S_l, directly governs the rate of flame propagation in premixed fuel/air systems, exerting a profound influence on the potential severity of explosion events (see, e.g., Di Sarli et al., 2009, 2012). S_l is a key parameter for comprehensively evaluating the

* Corresponding author.
E-mail address: valeria.disarli@stems.cnr.it (V. Di Sarli).

https://doi.org/10.1016/j.jlp.2024.105479
Received 10 July 2024; Received in revised form 27 October 2024; Accepted 2 November 2024
Available online 2 November 2024

safety implications of ethanol-ethyl acetate mixtures, with specific reference to vapor explosions. The integration of the concept of laminar burning velocity into risk assessment facilitates the development of tailored protocols aimed at effectively predicting, preventing, and mitigating explosions. Hence, this study endeavors to bridge this critical knowledge gap by examining the interaction between ethanol and ethyl acetate when burning together, through the production of new experimental and numerical data for the laminar burning velocity of ethanol, ethyl acetate, and ethanol-ethyl acetate mixtures in air. Experimental data were obtained from pressure time histories recorded during closed vessel explosion tests. Numerical data were obtained from simulations performed using three detailed chemical kinetic mechanisms developed, respectively, by the University of Bologna (Wako et al., 2022), by Ahmed et al. (2019), and by Dayma et al. (2012). These three mechanisms were selected based on their demonstrated robustness in capturing the low temperature chemistry of different oxygenated fuels across various reaction conditions. Their validation was performed here comparing computed data both with the newly produced experimental data and with experimental data retrieved from the literature (but only for ethanol and ethyl acetate). Motivated by some encouraging literature results (Di Sarli and Di Benedetto, 2007; Sileghem et al., 2012; Zhang et al., 2022), the ability of a Le Chatelier's mixing rule-like formula to predict the laminar burning velocity of ethanol-ethyl acetate mixtures was also assessed.

2. Methodology

2.1. Computations

The laminar burning velocity, S_l, of ethanol/, ethyl acetate/, and ethanol-ethyl acetate/air mixtures was computed using the code for modeling steady laminar one-dimensional premixed flames from the open source software package Cantera version 3.0.0 (Goodwin et al., 2023). Three different detailed chemical kinetic mechanisms were implemented into the code: the KiBo_MU mechanism (Wako et al., 2022), which is the manually upgraded (MU) version of the original KiBo mechanism developed at the University of Bologna for light alkenes (Pio et al., 2018); the mechanism developed by Ahmed et al. (2019) using AramcoMech 2.0 (Li et al., 2017) as a seed mechanism; and the mechanism proposed by Dayma et al. (2012). For these three mechanisms, Table 1 details the number of species, the number of reactions, and the validation conditions for calculations of S_l, in terms of fuel type, temperature, pressure, and (fuel/air) equivalence ratio, φ. All mechanisms were confirmed to be robust to the low temperature chemistry of oxygenated fuels over ranges of reaction conditions. Specifically, their ability to capture the experimental trends of S_l for different oxygenated fuels under wide ranges of reaction conditions was a good indicator that they could be used to investigate the chemistry of ethanol, ethyl acetate, and ethanol-ethyl acetate mixtures.

The compositions explored in the computations performed in this study are reported in Table 2. Temperature and pressure were set to 90 °C (363 K) and 1 atm, respectively.

Computations were run using a transient condition as a first attempt solution for the steady state condition. The following simulation criteria were used for solving steady state (ss) and transient state (ts) problems:

Table 2
Compositions explored in the computations performed in this study.

System	φ (−)
Ethanol/; Ethyl Acetate/; Ethanol-Ethyl Acetate/Air	0.6-1.7
System	**Ethanol Mole Fraction (−)**
Ethanol-Ethyl Acetate	0.25; 0.50; 0.75

absolute tolerance_ss $= 1.0 \times 10^{-8}$; relative tolerance_ss $= 1.0 \times 10^{-15}$; absolute tolerance_ts $= 1.0 \times 10^{-4}$; and relative tolerance_ts $= 1.0 \times 10^{-13}$. An adaptive grid was determined using the following criteria: maximum acceptable ratio among adjacent solutions (ratio) equal to 3; maximum first derivative for adjacent solutions (slope) equal to 0.06; and maximum acceptable second derivative for adjacent solutions (curve) equal to 0.12. The Soret effect and the multicomponent transport model were initially neglected to generate a first guess result and were subsequently considered for the final solution.

2.2. Experiments

Fig. 1 shows a schematic representation of the experimental setup used in this study for explosion tests. The core of this setup is the reactor, a closed cylindrical chamber (volume of 5 L and length-to-diameter ratio of around 3) made of AISI 316 stainless steel. This setup was used for explosion tests on vaporized (liquid) fuels in our previous works (Cammarota et al., 2012, 2019, 2022).

Spark ignition was provided at the center of the reactor using an electric arc produced by a high voltage power generator (25 kV DC, 5

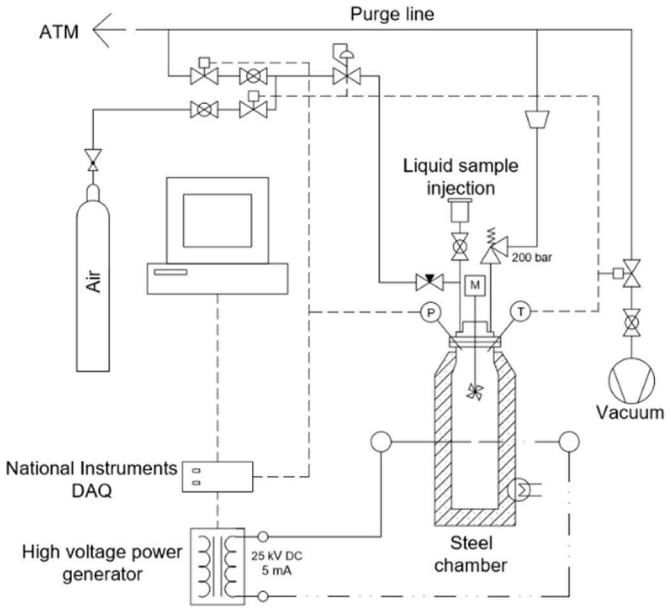

Fig. 1. Schematic representation of the experimental setup used in this study for explosion tests.

Table 1
The three detailed chemical kinetic mechanisms used in this study to compute the laminar burning velocity, S_l, of ethanol/, ethyl acetate/, and ethanol-ethyl acetate/air mixtures: number of species; number of reactions; validation conditions for calculations of S_l, in terms of fuel type, temperature, pressure, and (fuel/air) equivalence ratio, φ.

Mechanism	No. Species	No. Reactions	Validation Conditions for Calculations of S_l			
			Fuel Type	Temperature (K)	Pressure	φ (−)
KiBo_MU (Wako et al., 2022)	141	453	Formic acid	373-423	1 atm	0.8-1.3
Ahmed et al. (2019)	506	2809	Methyl acetate and ethyl acetate	298-338	1 atm	0.7-1.4
Dayma et al. (2012)	232	1845	C_4-C_7 ethyl esters	323-473	1-10 bar	0.7-1.5

mA — spark generator by Kühner (model KSEP 320)). The circuit was controlled by solid state relays through an electrical board. The spark gap was set to 6 mm, and the spark discharge time was adjusted to a value of 0.2-1.0 s. For pressure measurements, a high precision KULITE piezoelectric transducer (type ETS-IA-375M-350 BARA) was installed at the top of the reactor. A high resolution acquisition system (National Instruments USB-6251 — 1.25 MS/s) was employed. The initial temperature of the chamber was obtained using an external PID-controlled heater. The gas temperature was checked by a type K thermocouple placed at the center of the chamber.

Conditions were the same in both experiments and computations. However, explosion tests were performed only at $\varphi = 1.1$, i.e., the composition at which, according to calculations, S_l achieves its maximum value for all systems. At each condition, tests were run in triplicate.

Ethanol (purity ≥99.8%) and ethyl acetate (purity ≥99.8%) were purchased from Merck. Ethanol/, ethyl acetate/, and ethanol-ethyl acetate/air mixtures were obtained using the partial pressure methodology. The reactor was first heated to 90 °C and, after a vacuum of about 0.02 bar was achieved, the fuel or fuel mixture was fed to the vessel (in liquid form). Finally, air was added until the initial pressure of 1 bar was reached. A top rotating fan ensured good mixing of the reactants. Stirring was produced during the entire loading phase of the reactor. Ignition was provided 30 s after that stirring was stopped. This delay time allowed turbulence to decay, while preserving the homogeneous nature of the mixture.

Recorded pressure time histories were used to estimate the laminar burning velocity, S_l, for the systems investigated. Specifically, S_l was obtained from the time derivative of the flame radius, r_f, given by (Dahoe et al., 1996):

$$r_f = \left(\frac{3V}{4\pi}\right)^{1/3}\left[1-\left(\frac{P_0}{P}\right)^{1/\gamma}\left(\frac{P_{ex}-P}{P_{ex}-P_0}\right)\right]^{1/3} \quad (1)$$

where V is the vessel volume, P_0, P_{ex}, and P are the initial pressure, the peak pressure, and the actual pressure, respectively, and γ is the adiabatic coefficient of the unburned gas. The time derivative was

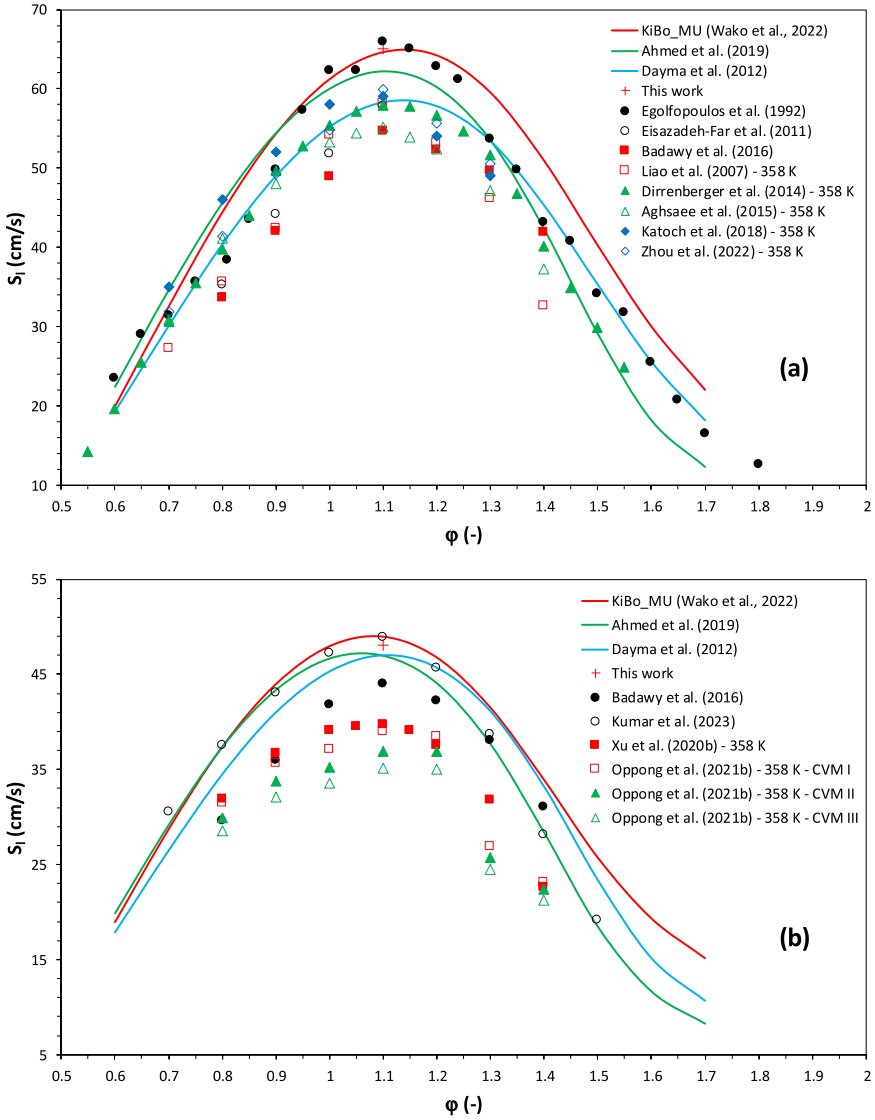

Fig. 2. Laminar burning velocity, S_l, versus equivalence ratio, φ, for (a) ethanol/ and (b) ethyl acetate/air: calculations performed using three different detailed chemical kinetic mechanisms (lines) and experimental data (symbols) — the latter also include the values of S_l estimated here from pressure time histories recorded during closed vessel explosion experiments (mean values represented by crosses). Legends: unless otherwise specified, the temperature conditions of the literature experiments are the same as those of this work (363 K); CVM stands for "constant volume method", and the labels CVM I, CVM II, and CVM III refer to the laminar burning velocity obtained with different burned mass fraction correlations (Oppong et al., 2021b).

determined considering a range of values for r_f where the effects of ignition ($r_f \geq 3$ cm) and vessel wall ($r_f \leq 6$ cm) on the flame propagation were both negligible, thus ensuring the flame radius to linearly increase with time. The standard deviation on S_l was always less than 1.5%. The validity of this simplified methodology (as well as of the experimental setup) for estimating S_l was already proved for ethanol (Cammarota et al., 2012).

3. Results and discussion

3.1. Ethanol and ethyl acetate

Fig. 2 shows the laminar burning velocity, S_l, of (a) ethanol/ and (b) ethyl acetate/air versus the equivalence ratio, φ, as obtained from computations performed using the three different detailed chemical kinetic mechanisms described in Sub-Section 2.1 (lines). In this figure, the experimental data retrieved from the literature for ethanol (Egolfopoulos et al., 1992; Liao et al., 2007; Eisazadeh-Far et al., 2011; Dirrenberger et al., 2014; Aghsaee et al., 2015; Badawy et al., 2016; Katoch et al., 2018; Zhou et al., 2022) and ethyl acetate (Badawy et al., 2016; Xu et al., 2020b; Oppong et al., 2021b; Kumar et al., 2023) are also shown (symbols). Unless otherwise specified in the legends, the temperature conditions of the literature experiments are the same as those of this work (363 K). In the legend of Fig. 2b, CVM stands for "constant volume method", and the labels CVM I, CVM II, and CVM III refer to the laminar burning velocity obtained with different burned mass fraction correlations (Oppong et al., 2021b).

The experimental data are rather scattered possibly owing to the different techniques/methodologies used to evaluate the laminar burning velocity in the various works. This is especially true in the case of ethyl acetate. However, regardless of the kinetic mechanism implemented into the Cantera software, reasonable agreement is found between calculations and experiments. Among other things, with both fuels, the characteristic bell shape of the experimental trends is well captured by the calculations and, as in the experiments, the computed curves are rather flat around the maximum, which occurs at $\varphi = 1.1$.

At $\varphi = 1.1$, explosion experiments were carried out on both ethanol and ethyl acetate, using the setup schematized in Fig. 1. Fig. 3 shows the pressure time histories recorded during such tests. These are the typical curves of low reactivity gaseous systems exploding in non-adiabatic closed cylindrical vessel (Di Benedetto et al., 2009; Di Sarli et al., 2014). Higher rate of explosion pressure rise is well evident for ethanol. This is a clear indication of its higher reactivity compared to ethyl acetate. To quantify the reactivity of these two fuels in terms of laminar burning velocity, the simplified methodology briefly discussed in Sub-Section 2.2 was applied to the recorded pressure time histories. Fig. 2 shows the results obtained (mean values represented by crosses). They are close to the experimental data that Egolfopoulos et al. (1992) and Kumar et al. (2023) produced for ethanol and ethyl acetate, respectively. In the case of ethyl acetate, the predictions of all three mechanisms agree well with both these experimental data. Conversely, in the case of ethanol, the KiBo_MU mechanism (Wako et al., 2022) provides the best agreement.

3.2. Ethanol-ethyl acetate mixtures

Fig. 4 shows the laminar burning velocity, S_l, of ethanol-ethyl acetate/air mixtures versus the equivalence ratio, φ, as obtained from computations performed using the three kinetic mechanisms developed, respectively, by (a) the University of Bologna (Wako et al., 2022), (b) Ahmed et al. (2019), and (c) Dayma et al. (2012) (solid lines). The red and black curves correspond to ethanol and ethyl acetate, respectively. The linear trends obtained by averaging the values of S_l calculated for ethanol and ethyl acetate according to their mole fractions in the fuel (ethanol-ethyl acetate) mixture

$$S_{l_{Linear}}(\varphi) = x_{Ethanol} \bullet S_{l\,Ethanol}(\varphi) + (1 - x_{Ethanol}) \bullet S_{l\,Ethyl\ Acetate}(\varphi) \quad (2)$$

are also shown (dashed lines). With all three mechanisms, the behavior of ethanol-ethyl acetate is bounded between the behaviors of ethanol and ethyl acetate, approaching the former/latter as the mixture is enriched in ethanol/ethyl acetate. In addition, the solid lines are (slightly) below the corresponding dashed lines (the maximum difference between the solid and dashed lines is around 2.4 cm/s — it is found with the mechanism by Ahmed et al. (2019)). This suggests that the interaction between ethanol and ethyl acetate in the mixtures gives rise to (weak) anti-synergistic effects with a consequent (slight) decrease in reactivity. Thus, while synergistic effects come into play with the flash point behavior of ethanol-ethyl acetate mixtures (Di Benedetto et al., 2018a), the same is not true with the combustion behavior. This is an important feature of ethanol-ethyl acetate systems.

Whatever the composition of the fuel mixture, S_l achieves its maximum value at $\varphi = 1.1$ with all three mechanisms. At this value of

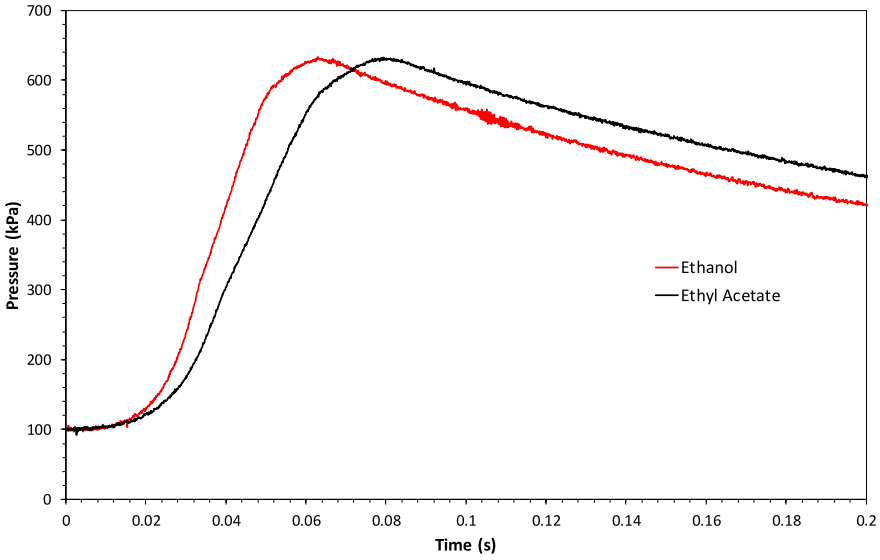

Fig. 3. Pressure time histories recorded during closed vessel explosion tests performed on ethanol/ and ethyl acetate/air ($\varphi = 1.1$), using the setup schematized in Fig. 1.

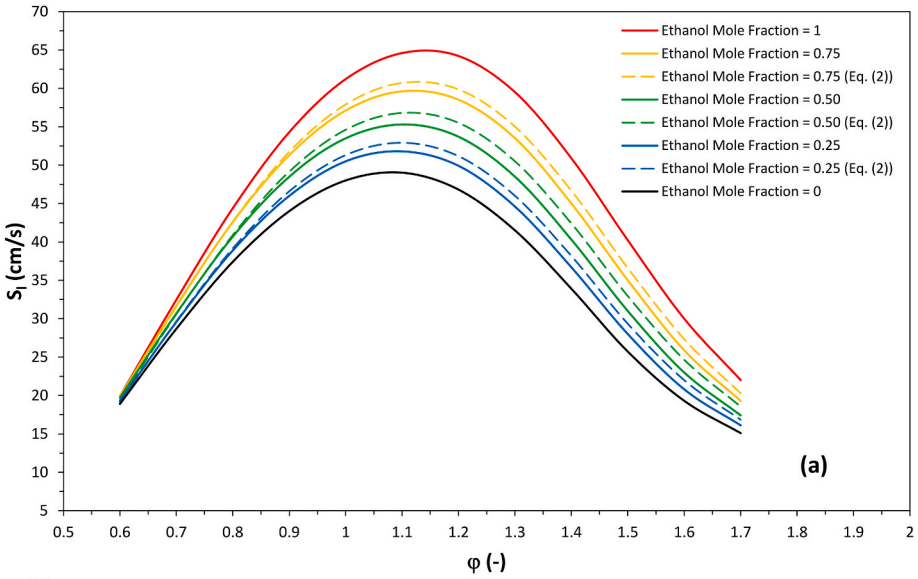

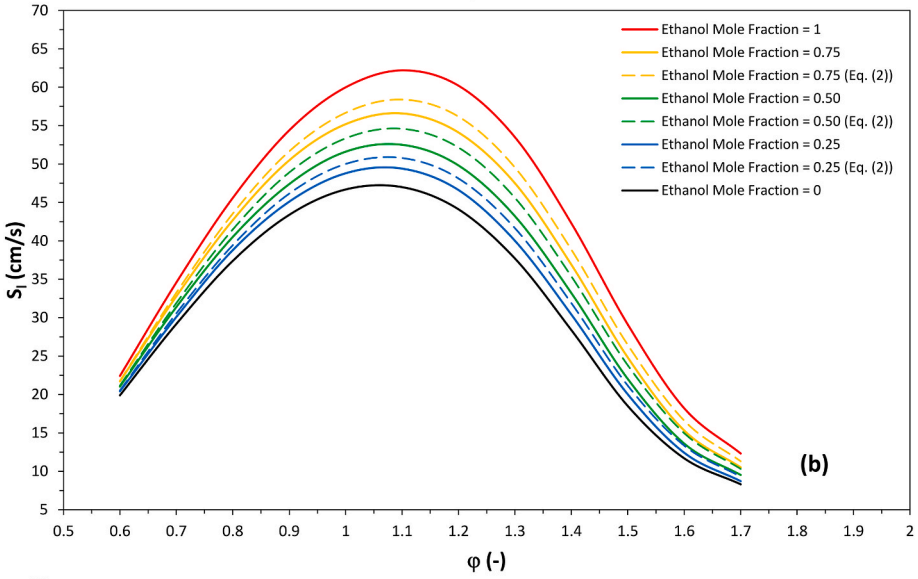

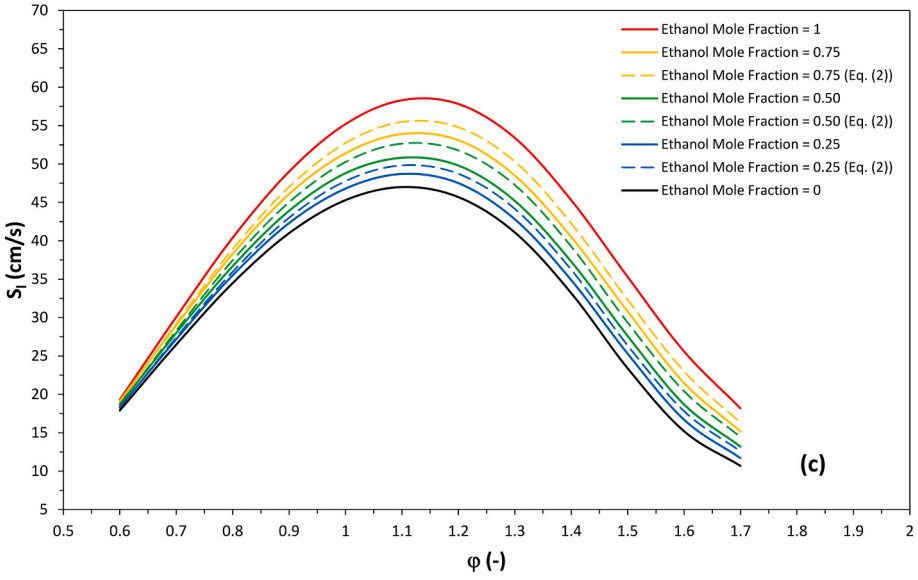

(caption on next page)

Fig. 4. Laminar burning velocity, S_l, versus equivalence ratio, φ, as calculated for ethanol-ethyl acetate/air at different ethanol mole fractions in the fuel mixture, using the three detailed chemical kinetic mechanisms developed, respectively, by (a) the University of Bologna (Wako et al., 2022), (b) Ahmed et al. (2019), and (c) Dayma et al. (2012) (solid lines). The red and black curves correspond to ethanol and ethyl acetate, respectively. The linear trends obtained by averaging the values of S_l calculated for ethanol and ethyl acetate according to their mole fractions in the fuel mixture (Eq. (2)) are also shown (dashed lines). (For interpretation of the references to color in this figure legend, the reader is referred to the Web version of this article.)

equivalence ratio, closed vessel explosion experiments were also carried out on ethanol-ethyl acetate mixtures. The methodology discussed in Sub-Section 2.2 and applied to the pressure time histories of ethanol and ethyl acetate was extended to their mixtures. Fig. 5 shows the values of S_l obtained from the application of this methodology (mean values represented by circles) as a function of the ethanol mole fraction in the fuel mixture, along with the values computed using the three different mechanisms (solid lines). In this figure, ethanol and ethyl acetate are also shown as extreme cases. The predictions obtained with the KiBo_MU mechanism (Wako et al., 2022) best agree with the experimental data.

In Fig. 5, the dotted line corresponds to the linear trend (Eq. (2)) calculated based on the experimental data of ethanol and ethyl acetate. As already seen with the computed data (Fig. 4), all experimental points fall (slightly) below the linear trend (the maximum difference between the measurements and the predictions of Eq. (2) is around 1.5 cm/s).

Zhang et al. (2022) measured the lower flammability limit (LFL) of ethanol-ethyl acetate mixtures — with mole fractions of ethanol in the fuel mixture varying in the range 0.1-0.9 — in air using a home-built experimental apparatus whose core is a spherical explosion chamber. They found that Le Chatelier's rule predicts well the values of LFL obtained. The ability of a Le Chatelier's mixing rule-like formula

$$S_{l_{Le\ Chatelier}}(\varphi) = \frac{1}{x_{Ethanol}/S_{lEthanol}(\varphi) + (1 - x_{Ethanol})/S_{lEthyl\ Acetate}(\varphi)} \quad (3)$$

to predict the laminar burning velocity of ethanol-ethyl acetate mixtures was also assessed here. In Di Sarli and Di Benedetto (2007), this empirical formula was used to predict the laminar burning velocity of hydrogen-methane/air mixtures obtained from simulations performed with a detailed chemical kinetic mechanism. At lean and stoichiometric conditions, good agreement was found regardless of the fuel composition, whereas at rich conditions, good agreement was found only for mole fractions of hydrogen in the fuel lower than 0.7. Analogously, Sileghem et al. (2012) showed that, for the laminar burning velocity of ethanol-*n*-heptane/air mixtures (with mole fraction of ethanol in the fuel equal to 0.5), this formula works well mainly at lean and stoichiometric conditions. However, at $\varphi > 1$, the maximum difference between measured and predicted values is only 2 cm/s. In Fig. 5, the dashed line corresponds to the trend calculated using Eq. (3) (and the experimental data of ethanol and ethyl acetate). It is seen that the predictions of this equation agree well with the experimental data.

The ability of Eq. (3) to predict the laminar burning velocity of ethanol-ethyl acetate mixtures was also assessed in relation to the computed values of this parameter. For all values of equivalence ratio (0.6-1.7) and ethanol mole fraction in the fuel mixture (0.25, 0.50, and 0.75) investigated in this work, Fig. 6 shows the laminar burning velocity predicted using Eq. (3), $S_{l\_Eq.\ (3)}$, as a function of the corresponding laminar burning velocity computed using the Cantera software, $S_{l\_Cantera}$, with the three different kinetic mechanisms. For each mechanism, the root mean square error, RMSE, and the coefficient of determination, R^2, are also reported. According to this figure, with all three mechanisms, Eq. (3) also predicts values of S_l that closely match the computed data. This is true regardless of the composition (i.e., equivalence ratio and ethanol mole fraction in the fuel mixture) of the system. The predictive ability of Eq. (3) shown in Fig. 5 and Fig. 6 suggests that the kinetic coupling between the two fuels is of minor importance to the laminar burning velocity of ethanol-ethyl acetate mixtures and the flame temperature mostly governs this parameter (Hirasawa et al., 2002). While the plots of Fig. 7 highlight the strong dependence of S_l on the adiabatic flame temperature, T_{ad}, at different equivalence ratios, Fig. 8 provides further proof of the dominant role of the flame temperature, showing the improvement of the predictive ability when, in Eq. (2), the mole fractions are replaced by the energy fractions (Sileghem et al., 2012)

$$S_{l_{Linear}}(\varphi) = \alpha_{Ethanol} \bullet S_{lEthanol}(\varphi) + (1 - \alpha_{Ethanol}) \bullet S_{lEthyl\ Acetate}(\varphi) \quad (4)$$

with

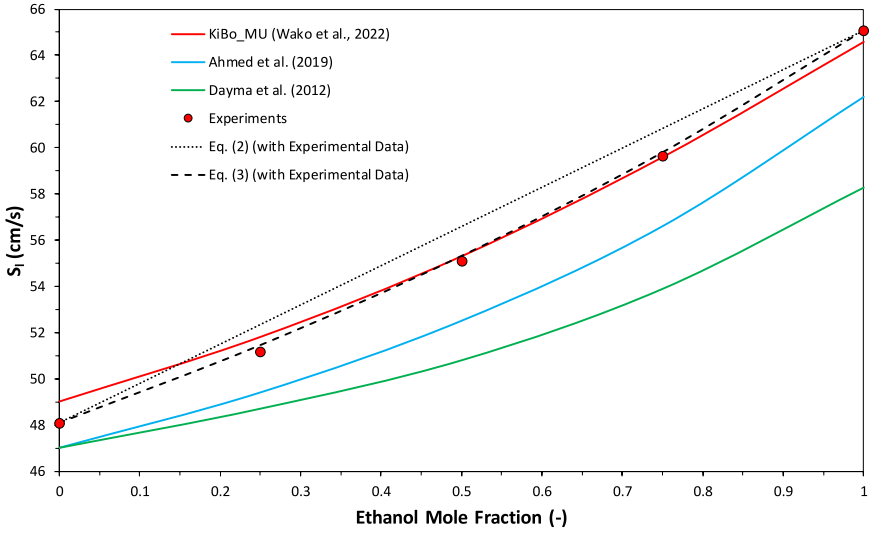

Fig. 5. Laminar burning velocity, S_l, versus ethanol mole fraction in the fuel (ethanol-ethyl acetate) mixture as obtained from closed vessel explosion experiments (mean values represented by circles) and computed using different chemical kinetic mechanisms (solid lines) ($\varphi = 1.1$). The dotted and dashed lines correspond to the predictions calculated using Eq. (2) and Eq. (3), respectively, with the experimental data of ethanol and ethyl acetate.

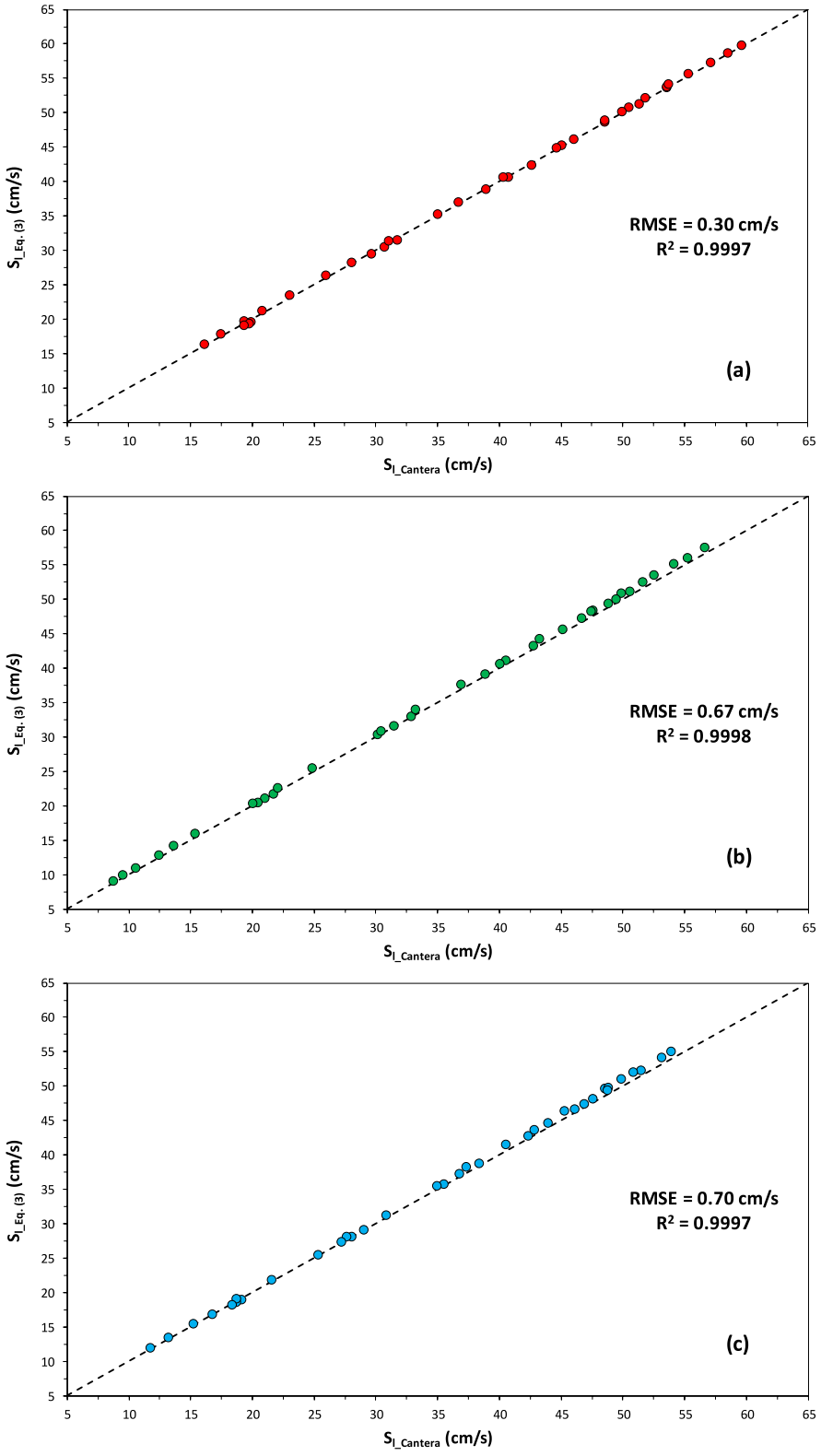

Fig. 6. Laminar burning velocity of ethanol-ethyl acetate/air mixtures predicted using Eq. (3), $S_{l\_Eq.\ (3)}$, as a function of the corresponding laminar burning velocity computed using the Cantera software, $S_{l\_Cantera}$, with the three different detailed chemical kinetic mechanisms developed, respectively, by (a) the University of Bologna (Wako et al., 2022), (b) Ahmed et al. (2019), and (c) Dayma et al. (2012). All values of equivalence ratio (0.6-1.7) and ethanol mole fraction in the fuel mixture (0.25, 0.50, and 0.75) were considered. For each mechanism, the root mean square error, RMSE, and the coefficient of determination, R^2, are also reported.

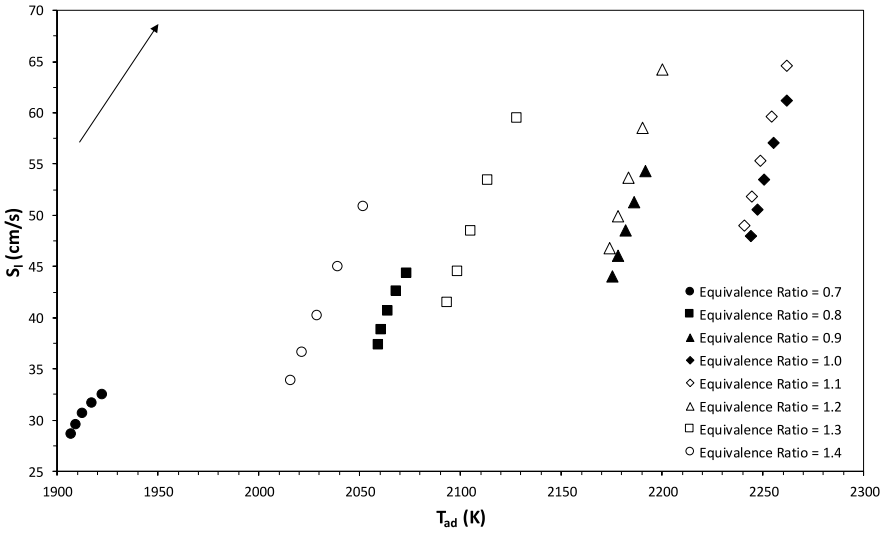

Fig. 7. Laminar burning velocity, S_l, versus adiabatic flame temperature, T_{ad}, at different equivalence ratios. The arrow indicates the trend of increasing ethanol mole fraction in the fuel mixture (from 0 (only ethyl acetate) to 1 (only ethanol)). (Computations run using the KiBo_MU mechanism (Wako et al., 2022).)

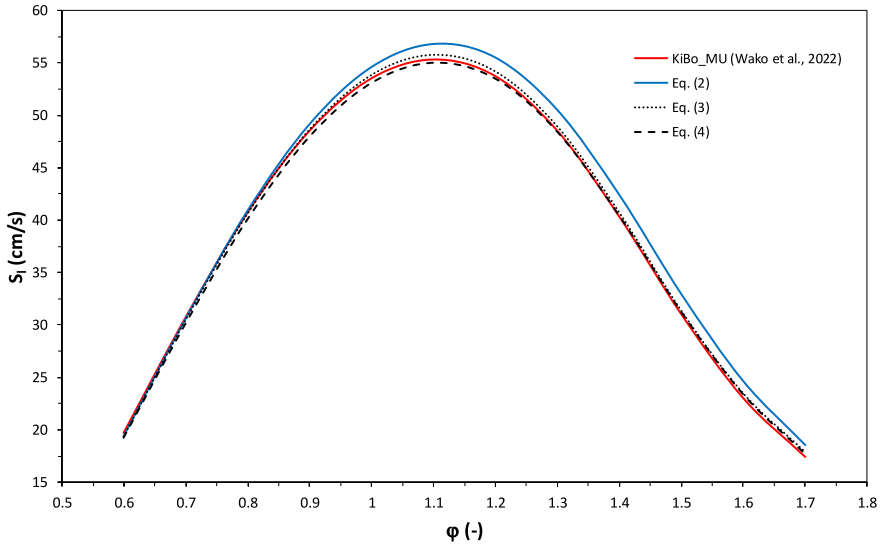

Fig. 8. Laminar burning velocity, S_l, versus equivalence ratio, φ, as calculated for ethanol-ethyl acetate (ethanol mole fraction in the fuel mixture equal to 0.50) in air using the KiBo_MU mechanism (Wako et al., 2022) (red line), along with the trends obtained by averaging the values of S_l calculated for ethanol and ethyl acetate according to their mole fractions (Eq. (2)) (blue line) and energy fractions (Eq. (4)) (dashed line) in the fuel mixture. For the sake of comparison, the predictions of Eq. (3) are also shown (dotted line). (For interpretation of the references to color in this figure legend, the reader is referred to the Web version of this article.)

$$\alpha_{Ethanol} = \frac{x_{Ethanol} \bullet \text{Heat of Combustion}_{Ethanol}}{x_{Ethanol} \bullet \text{Heat of Combustion}_{Ethanol} + (1 - x_{Ethanol}) \bullet \text{Heat of Combustion}_{Ethyl\ Acetate}} \quad (5)$$

Fig. 8 also shows the predictions of Eq. (3). Based on these results, the predictive ability of Eq. (4) is similar to that of Eq. (3). However, Eq. (3) has the greater simplicity as an advantage, as it does not require the determination of the heat of combustion of the fuels constituting the mixture.

4. Conclusions

The main conclusions drawn from the results obtained in this work are summarized as follows. First, regardless of the kinetic mechanism used to calculate the laminar burning velocity, S_l, of ethanol-ethyl acetate mixtures in air, reasonable agreement is found between computed and experimental data, including experimental data retrieved from the literature for ethanol and ethyl acetate. Secondly, the values of S_l for ethanol-ethyl acetate are always smaller than those obtained by averaging the corresponding values of ethanol and ethyl acetate according to

their mole proportions in the fuel mixture — in other words, anti-synergist effects come into play when ethanol and ethyl acetate burn together. Finally, a simple Le Chatelier's mixing rule-like formula is proved to predict values of S_l that closely match both computed and experimental data, suggesting that the nature of the interaction between ethanol and ethyl acetate is predominantly thermal rather than chemical. This formula could also be used to predict the explosion severity on the basis of which to design adequate mitigation measures.

5. Funding

This research did not receive any specific grant from funding agencies in the public, commercial, or not-for-profit sectors.

CRediT authorship contribution statement

Ernesto Salzano: Writing – review & editing, Validation, Supervision. **Benedetta Anna De Liso:** Validation, Investigation, Data curation. **Francesco Cammarota:** Validation, Investigation, Data curation. **Valeria Di Sarli:** Writing – review & editing, Writing – original draft, Visualization, Validation, Supervision, Investigation, Formal analysis, Data curation, Conceptualization.

Declaration of competing interest

The authors declare that they have no known competing financial interests or personal relationships that could have appeared to influence the work reported in this paper. Ernesto Salzano is an Editorial Board Member for the *Journal of Loss Prevention in the Process Industries* and was not involved in the editorial review or the decision to publish this article.

Acknowledgements

The authors wish to thank Ernesto Marinò for his technical support in the experimental activity.

Data availability

Data will be made available on request.

References

Aghsaee, M., Nativel, D., Bozkurt, M., Fikri, M., Chaumeix, N., Schulz, C., 2015. Experimental study of the kinetics of ethanol pyrolysis and oxidation behind reflected shock waves and in laminar flames. Proc. Combust. Inst. 35, 393–400. https://doi.org/10.1016/j.proci.2014.05.063.

Ahmed, A., Pitz, W.J., Cavallotti, C., Mehl, M., Lokachari, N., Nilsson, E.J.K., Jui-Yang, W., Konnov, A.A., Wagnon, S.W., Bingjie, C., Zhandong, W., Seonah, K., Curran, H.J., Klippenstein, S.J., Roberts, W.L., Sarathy, S.M., 2019. Small ester combustion chemistry: computational kinetics and experimental study of methyl acetate and ethyl acetate. Proc. Combust. Inst. 37, 419–428. https://doi.org/10.1016/j.proci.2018.06.178.

Badawy, T., Williamson, J., Xu, H., 2016. Laminar burning characteristics of ethyl propionate, ethyl butyrate, ethyl acetate, gasoline and ethanol fuels. Fuel 183, 627–640. https://doi.org/10.1016/j.fuel.2016.06.087.

Cammarota, F., Di Benedetto, A., Di Sarli, V., Salzano, E., 2012. The effect of hydrogen addition on the explosion of ethanol/air mixtures. Chemical Engineering Transactions 26, 405–410. https://doi.org/10.3303/CET1226068.

Cammarota, F., Di Benedetto, A., Di Sarli, V., Salzano, E., 2019. Influence of initial temperature and pressure on the explosion behavior of *n*-dodecane/air mixtures. J. Loss Prev. Process. Ind. 62, 103920. https://doi.org/10.1016/j.jlp.2019.103920.

Cammarota, F., Di Sarli, V., Salzano, E., 2022. Explosion behavior of ethanol-ethyl acetate/air mixtures. Chemical Engineering Transactions 91, 511–516. https://doi.org/10.3303/CET2291086.

Crowl, D.A., 2003. Understanding Explosions. American Institute of Chemical Engineers, New York. https://onlinelibrary.wiley.com/doi/book/10.1002/9780470925287.

Dahoe, A.E., Zevenbergen, J.F., Lemkowitz, S.M., Scarlett, B., 1996. Dust explosions in spherical vessels: the role of flame thickness in the validity of the 'cube-root law'. J. Loss Prev. Process. Ind. 9, 33–44. https://doi.org/10.1016/0950-4230(95)00054-2.

Dayma, G., Halter, F., Foucher, F., Mounaim-Rousselle, C., Dagaut, P., 2012. Laminar burning velocities of C_4–C_7 ethyl esters in a spherical combustion chamber: experimental and detailed kinetic modeling. Energy & Fuels 26, 6669–6677. https://doi.org/10.1021/ef301254q.

Di Benedetto, A., Di Sarli, V., Salzano, E., Cammarota, F., Russo, G., 2009. Explosion behavior of $CH_4/O_2/N_2/CO_2$ and $H_2/O_2/N_2/CO_2$ mixtures. Int. J. Hydrogen Energy 34, 6970–6978. https://doi.org/10.1016/j.ijhydene.2009.05.120.

Di Benedetto, A., Sanchirico, R., Di Sarli, V., 2018a. Flash point of flammable binary mixtures: synergistic behavior. J. Loss Prev. Process. Ind. 52, 1–6. https://doi.org/10.1016/j.jlp.2018.01.005.

Di Benedetto, A., Sanchirico, R., Di Sarli, V., 2018b. Effect of pressure on the flash point of various fuels and their binary mixtures. Process Saf. Environ. Protect. 116, 615–620. https://doi.org/10.1016/j.psep.2018.03.022.

Di Sarli, V., Di Benedetto, A., 2007. Laminar burning velocity of hydrogen–methane/air premixed flames. Int. J. Hydrogen Energy 32, 637–646. https://doi.org/10.1016/j.ijhydene.2006.05.016.

Di Sarli, V., Di Benedetto, A., Russo, G., 2009. Using Large Eddy Simulation for understanding vented gas explosions in the presence of obstacles. J. Hazard Mater. 169, 435–442. https://doi.org/10.1016/j.jhazmat.2009.03.115.

Di Sarli, V., Di Benedetto, A., Long, E.J., Hargrave, G.K., 2012. Time-Resolved Particle Image Velocimetry of dynamic interactions between hydrogen-enriched methane/air premixed flames and toroidal vortex structures. Int. J. Hydrogen Energy 37, 16201–16213. https://doi.org/10.1016/j.ijhydene.2012.08.061.

Di Sarli, V., Cammarota, F., Salzano, E., 2014. Explosion parameters of wood chip-derived syngas in air. J. Loss Prev. Process. Ind. 32, 399–403. https://doi.org/10.1016/j.jlp.2014.10.016.

Dirrenberger, P., Glaude, P.A., Bounaceur, R., Le Gall, H., Pires da Cruz, A., Konnov, A. A., Battin-Leclerc, F., 2014. Laminar burning velocity of gasolines with addition of ethanol. Fuel 115, 162–169. https://doi.org/10.1016/j.fuel.2013.07.015.

Egolfopoulos, F.N., Du, D.X., Law, C.K., 1992. A study on ethanol oxidation kinetics in laminar premixed flames, flow reactors, and shock tubes. Symposium (International) on Combustion 24, 833–841. https://doi.org/10.1016/S0082-0784(06)80101-3.

Eisazadeh-Far, K., Moghaddas, A., Al-Mulki, J., Metghalchi, H., 2011. Laminar burning speeds of ethanol/air/diluent mixtures. Proc. Combust. Inst. 33, 1021–1027. https://doi.org/10.1016/j.proci.2010.05.105.

Goodwin, D.G., Moffat, H.K., Schoegl, I., Speth, R.L., Weber, B.W., 2023. Cantera: an object-oriented software toolkit for chemical kinetics, thermodynamics, and transport processes (3.0.0). Zenodo. https://doi.org/10.5281/zenodo.8137090.

Hirasawa, T., Sung, C.J., Joshi, A., Yang, Z., Wang, H., Law, C.K., 2002. Determination of laminar flame speeds using digital particle image velocimetry: binary fuel blends of ethylene, *n*-butane, and toluene. Proc. Combust. Inst. 29, 1427–1434. https://doi.org/10.1016/S1540-7489(02)80175-4.

Katoch, A., Millán-Merino, A., Kumar, S., 2018. Measurement of laminar burning velocity of ethanol-air mixtures at elevated temperatures. Fuel 231, 37–44. https://doi.org/10.1016/j.fuel.2018.05.083.

Kumar, R., Priyadarshani Padhi, U., Kumar, S., 2023. Laminar burning velocity measurements of ethyl acetate at higher mixture temperatures. Fuel 338, 127278. https://doi.org/10.1016/j.fuel.2022.127278.

Li, Q., Cheng, Y., Huang, Z., 2015. Comparative assessment of the explosion characteristics of alcohol–air mixtures. J. Loss Prev. Process. Ind. 37, 91–100. https://doi.org/10.1016/j.jlp.2015.07.003.

Li, Y., Zhou, C.-W., Somers, K.P., Zhang, K., Curran, H.J., 2017. The oxidation of 2-butene: a high pressure ignition delay, kinetic modeling study and reactivity comparison with isobutene and 1-butene. Proc. Combust. Inst. 36, 403–411. https://doi.org/10.1016/j.proci.2016.05.052.

Liao, S.Y., Jiang, D.M., Huang, Z.H., Zeng, K., Cheng, Q., 2007. Determination of the laminar burning velocities for mixtures of ethanol and air at elevated temperatures. Appl. Therm. Eng. 27, 374–380. https://doi.org/10.1016/j.applthermaleng.2006.07.026.

Lin, J.-H., Liu, L.-Y., Yang, M.-H., Lee, M.-H., 2004. Ethyl acetate/ethyl alcohol mixtures as an alternative to Folch reagent for extracting animal lipids. J. Agric. Food Chem. 52, 4984–4986. https://doi.org/10.1021/jf049360m.

Liu, Y., Liu, W., Liao, H., Ashan, H., Zhou, W., Xu, C., 2022. An experimental and a kinetic modelling study of ethanol/acetone/ethyl acetate mixtures. Energies 15, 2992. https://doi.org/10.3390/en15092992.

Mitu, M., Brandes, E., 2017. Influence of pressure, temperature and vessel volume on explosion characteristics of ethanol/air mixtures in closed spherical vessels. Fuel 203, 460–468. https://doi.org/10.1016/j.fuel.2017.04.124.

Ning, X., Zhang, Z., Zheng, K., Wang, X., Wang, J., 2023. Experimental and numerical studies on the explosion characteristics of ethanol–air mixtures under aviation conditions. Fire 6, 349. https://doi.org/10.3390/fire6090349.

Oppong, F., Zhongyang, L., Li, X., Xu, C., 2021a. Investigations on explosion characteristics of ethyl acetate. J. Loss Prev. Process. Ind. 70, 104409. https://doi.org/10.1016/j.jlp.2021.104409.

Oppong, F., Zhongyang, L., Li, X., Xu, C., 2021b. Investigations on laminar premixed flame characteristics of ethyl acetate. Combust. Flame 230, 111454. https://doi.org/10.1016/j.combustflame.2021.111454.

Pio, G., Palma, V., Salzano, E., 2018. Comparison and validation of detailed kinetic models for the oxidation of light alkenes. Ind. Eng. Chem. Res. 57, 7130–7135. https://doi.org/10.1021/acs.iecr.8b01377.

Sileghem, L., Vancoillie, J., Demuynck, J., Galle, J., Verhelst, S., 2012. Alternative fuels for spark-ignition engines: mixing rules for the laminar burning velocity of gasoline–alcohol blends. Energy & Fuels 26, 4721–4727. https://doi.org/10.1021/ef300393h.

Wako, F.M., Pio, G., Salzano, E., 2022. Modeling formic acid combustion. Energy & Fuels 36, 14382–14392. https://doi.org/10.1021/acs.energyfuels.2c03249.

Xu, C., Wu, S., Li, Y., Chu, S., Wang, C., 2020a. Explosion characteristics of hydrous bio-ethanol in oxygen-enriched air. Fuel 271, 117604. https://doi.org/10.1016/j.fuel.2020.117604.

Xu, C., Wu, S., Oppong, F., Xie, C., Wei, L., Zhou, J., 2020b. Experimental and numerical studies of laminar flame characteristics of ethyl acetate with or without hydrogen addition. Int. J. Hydrogen Energy 45, 20391–20399. https://doi.org/10.1016/j.ijhydene.2019.12.141.

Zhang, K., Gao, W., Li, Y., Zhang, Z., Shang, S., Zhang, C., Chen, X., Sun, K., 2022. Lower flammability limits of ethanol, acetone and ethyl acetate vapor mixtures in air. J. Loss Prev. Process. Ind. 74, 104676. https://doi.org/10.1016/j.jlp.2021.104676.

Zhou, J., Lu, C., Xu, C., Yu, Z., 2022. Experimental and numerical study on the effect of hydrogen addition on laminar burning velocity of ethanol–air mixtures. Energies 15, 3114. https://doi.org/10.3390/en15093114.